Journal of Aeronautical
-Science and Engineering-, Vol.3

August 25, 2015

Design of a Small Unmanned Aircraft

Kung Zi Yang, [a,*] and Ir. Dr. Istas Fahrurrazi Nusyirwan,[a,**]

[a)]*Department of Aeronautical Engineering, Faculty of Mechanical Engineering, Universiti Teknologi Malaysia, Skudai, Malaysia*

Corresponding author: *zy.yang_92@hotmail.com*[*], *istaz@mail.fkm.utm.my*[**]

Paper History

Received: 19-August-2015
Received in revised form: 20-August-2015
Accepted: 25-August-2015

ABSTRACT

A part of an undergraduate project, it is essential to understand the design process of an aircraft. The one-year project aims to design and fabricate a remotely controlled (RC) aircraft that is equipped with stabilization system. The work starts from the preliminary design process, i.e. sizing and weight estimation and airfoil selection. This is followed with the identification of important aerodynamic parameters. The identification uses several methods such as vortex lattice method and computational fluid dynamic analysis. The aerodynamic parameters are determined the performance of the aircraft and identifies the type of propulsion system needed. The stability of the aircraft uses linearized method to identify the stability characteristic of the aircraft. A prototype was built using low-cost materials and an off-the-shelf auto-stabilization system was able to stabilize the aircraft during the flight test. Post flight-test analysis are also conducted for verification.

KEY WORDS: *Aircraft Design Process; Aerodynamic Analysis; Performance Analysis; Stability Analysis.*

NOMENCLATURE

$\left(\frac{C_L{}^3}{C_D{}^2}\right)$	Lift power of 1.5 to Drag Ratio
$\left(\frac{C_L}{C_D}\right)$	Lift to Drag Ratio
$C_{l,0}{}_{cg}$	Rolling Moment Coefficient at zero beta
$C_{m,0}{}_{cg}$	Pitching Moment Coefficient at zero effective alpha
$C_{n,0}{}_{cg}$	Yawing Moment Coefficient at zero beta
C_D	Drag Coefficient
C_L	Lift Coefficient
P_0	Power Output
P_R	Power Required
P_a	Power Available
P_{excess}	Excess Power
$\frac{R}{C}$	Rate of Climb
S_w	Wing Span
U_{el}	Voltage Input
V_∞	Free stream Velocity
W_0	Aircraft Weight
$\dot{x}$	Derivatives State Vector
η_c	Control Vector
η_{prop}	Propeller Efficiency
η_{sys}	Circuit System Efficiency
$\frac{\partial C_{l_{cg}}}{\partial \beta}$	Roll Moment Curve Slope
$\frac{\partial C_{m_{cg}}}{\partial \alpha_e}$	Pitching Moment Curve Slope
$\frac{\partial C_{n_{cg}}}{\partial \beta}$	Yaw Moment Curve Slope
ΔC_{el}	Battery Capacity
A	Matrix A Aircraft Dynamic Characteristic
B	Matrix B Aircraft Dynamic Characteristic
E	Endurance
R	Range (km)
α	Alpha, Angle-of-attack
x	State Vector
ρ	Density

1.0 INTRODUCTION

An RC aircraft is well comparable with mini UAV and radio controlled model airplane in term of size and weight. According to Parsch [1] a mini UAV is approximately in range of 1m to 3m wing span. The main difference between these airplanes is the

mission to be carried out and the fundamental avionic employed. The main function of the propulsion system of the aircraft is to drive the aircraft up to the sky at a certain altitude. Then the power will be switch off and gliding flight is performed. Normally, gliding flight can be either performed by manually controlled or self-autonomous controlled. Manually controlled is referring to radio controlled by operator at ground station whereas autonomous controlled is referring to augmented system controlled by the integrated microprocessor.

2.0 PROJECT OVERVIEW

2.1 Objectives

The targets of this project are to exhibit a proper design process flow where involve engineering basics, such as analytical aerodynamic characteristics, preliminary performance analysis and stability analysis. Besides that, the project aims to develop a simple fabrication method to build the aircraft using low-cost materials. Flight tests provide important data for verification.

The design process of an aircraft follows the steps in Figure 1. Each step requires a thorough analysis through the literature and established methods. It is noted that the design process in an iterative process. However, due to time constraint, the iteration is not possible.

3.0 CONCEPTUAL DESIGN

3.1 Weight Estimation and Initial Sizing

Based on Raymer [3] and a parametric study on 29 existing similar category airplanes, the initial sizing is estimated according to the sizing procedure. The aircraft is expected to have high aspect ratio. The aspect ratio of 10 is used as reference. The minimum wing chord is 0.18m. These two values can be used to identify the other geometry sizing. Table 1 shows the initial sizing of the aircraft.

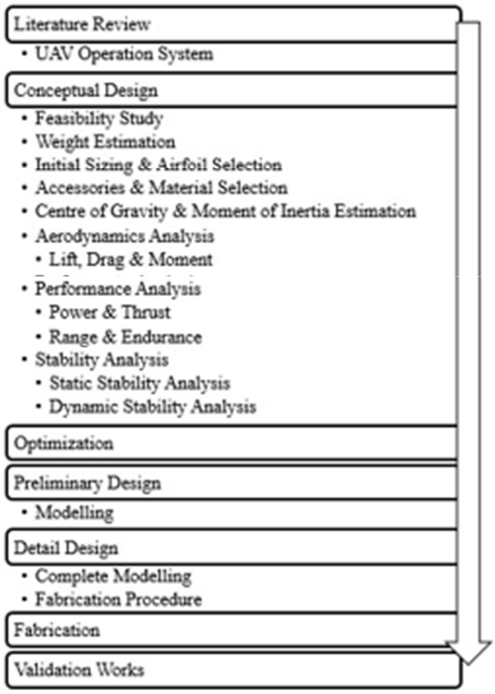

Figure 1: Design Process Flow, Raymer (2006)

Table 1: Initial Sizing and Weight Estimations

Parameter	Description
Wing MAC	0.18 m
Wing Span	1.8 m
Wing Aspect Ratio	10
Aileron Chord	0.045 m
Aileron Span	0.72 m
Horizontal Tail MAC	0.075 m
Horizontal Tail Span	0.45 m
Horizontal Tail Aspect Ratio	6
Elevator Chord	0.03 m
Elevator Span	0.45 m
Horizontal Tail Arm	0.86 m
Vertical Tail MAC	0.08 m
Vertical Tail Span	0.17 m
Vertical Tail Aspect Ratio	2.131 m
Rudder Chord	0.04 m
Rudder Span	0.17 m
Vertical Tail Arm	0.86 m
Fuselage length	1.32 m
Maximum Take-off Weight	1.15 kg

High wing configuration is chosen to increase the longitudinal stability of the aircraft. Rectangular wing configuration is used so that to ease fabrication process. Moreover, a conventional tail is used since this configuration is widely used and simple to fabricate. The propulsion system is pusher type. Figure 2 shows the conceptual drawing of the aircraft.

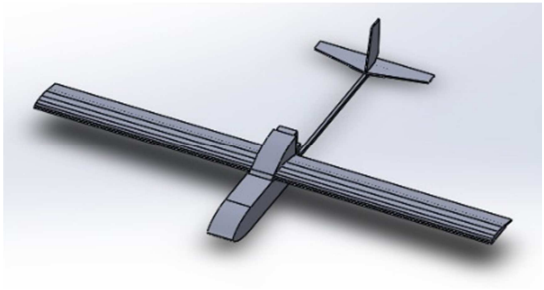

Figure 2: Conceptual Design Drawing.

3.2. Airfoil Selection

UIUC airfoil database [5] gives a wide range of airfoils for different usage, in this study, the selected airfoil for the wing has to be easy to fabricate. Clark-Y airfoil is selected due to flat surface at lower region. Flat sheet foams are used to approximate the upper curvature whereas the trailing edge is half done. Figure 3 shows the difference of Clark-Y airfoil and fabricated airfoil.

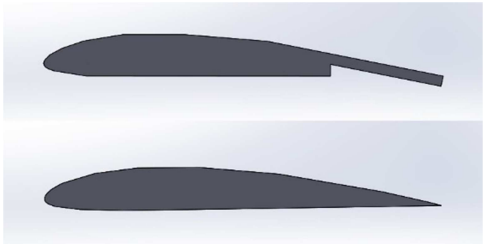

Figure 3: Fabricated airfoil (upper) and Clark-Y airfoil (lower).

4.0 AERODYNAMIC ANALYSIS

4.1 Comparing XFLR5 and ANSYS – Fluent Software

The XFLR5 software is widely used in aircraft design [2] and the data computed is in agreement with the XFOIL software invented by Mark Drela [10]. ANSYS-Fluent is commercial fluid dynamic computational software that calculates the flow around a test subject. The correlation between two software are determined so that to obtained more realistic data and justified the setup used in ANSYS – Fluent. Figure 4 shows the correlation between both of the software.

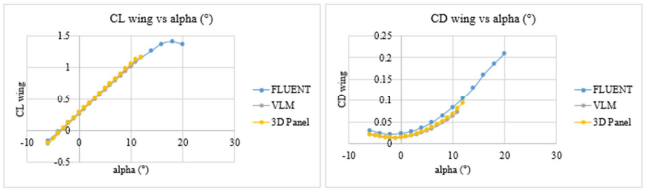

Figure 4: Correlation between XFLR5 and ANSYS – Fluent

The result obtained shows that both software correlate well with each other and by using the same setup in ANSYS – Fluent, the aerodynamic characteristics of other model can be determined.

4.2 Comparing Clark-Y and Modified Clark-Y Airfoil

Modified Clark-Y airfoil refers to the approximation of upper curvature with several flat surface. Figure 5 shows the difference between the Clark-Y and Modified Clark-Y airfoil and the result obtained is presented in Figure 6.

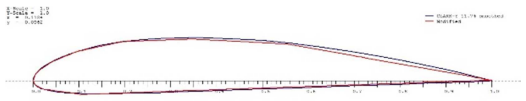

Figure 5: Clark-Y (blue) and Modified Clark-Y airfoil (red)

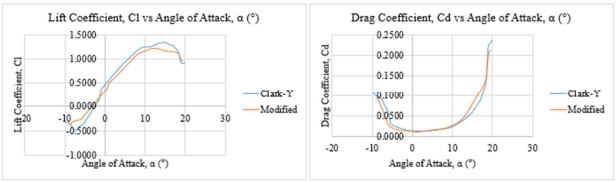

Figure 6: Comparing Clark-Y and Modified Clark-Y airfoil

The results obtained shows that the general curve shifted to positive region and this indicates that by applying an angle of incidence in wing design using modified Clark-Y would regain the aerodynamic characteristic of the Clark-Y wing design.

4.3 Aerodynamic Analysis Comparing Fabricated and Modified Clark-Y wing model

Due to limitation of fabrication, the aerodynamic characteristic of fabricated wing (shown in upper region of Figure 3) is required to be determined so that to check for the correlation with modified Clark-Y wing. The obtained results are shown in Figure 7.

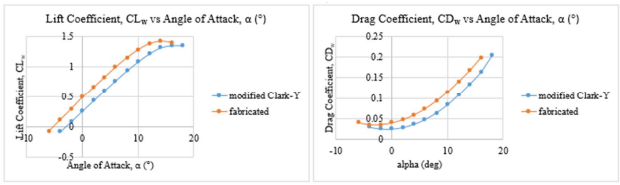

Figure 7: Comparing modified Clark-Y and fabricated wing

The result shows that the fabricated wing design is in agreement with the modified Clark-Y however the general trend of the data shifted to the left.

4.4 Aerodynamic Data for Aircraft

Using similar configuration in ANSYS – Fluent, the aerodynamic parameters of the aircraft can be determined. Figure 8 shows the aerodynamic characteristic of the aircraft. The reference airspeed can be calculated by using equation (1).

$$V_\infty = \sqrt{\frac{W_0}{\frac{1}{2}\rho S_W C_L}} \quad (1)$$

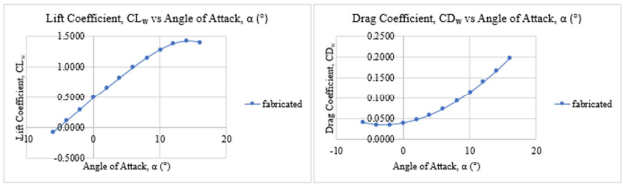

Figure 8: Lift coefficient and drag coefficient of aircraft

Pitching moment coefficient of the aircraft can be determined by considering two conditions, gliding flight and powered flight. The center of gravity is located approximately at the wing quarter chord, i.e. 0.05 m from the leading edge. The thrust available is estimated by using MotoCalc (commercial software) [4]. The obtained results are shown in Figure 9.

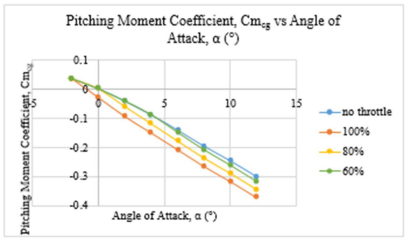

Figure 9: Pitching moment diagram

Yawing moment and rolling moment coefficient is determined using ANSYS – Fluent software. The obtained results are shown in Figure 10. Both rolling and yawing moments with respect to the sideslip angle show that the aircraft has some of degree of stability.

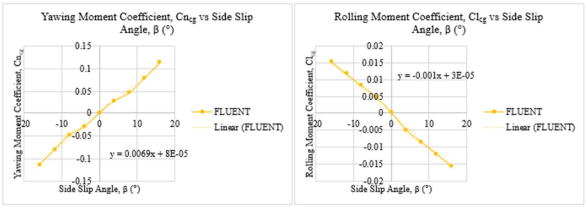

Figure 10: Yawing and rolling moment coefficient

5.0 PERFORMANCE ANALYSIS

5.1 Drag Polar

Drag polar is obtained by plotting lift coefficient versus drag coefficient. The obtained results are shown in Figure 11.

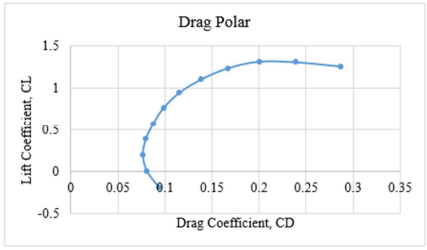

Figure 11: Drag polar

5.2 Power

A high-torque-low-rotational-speed electric motor is used so that to perform a low speed flight. The propulsion system specification is listed in Table 2.

Table 2: Propulsion system specifications

Electric motor	Emax XA - 2215
General power	180W
RPM	980kV
Battery capacity	LiPo battery 11.1V 2150mAh 30c
Propeller size	APC 10” x 4.7”

The motor performance is modeled using a commercial software called MotoCalc [4]. The software considers all the conditions of motor power output and these include the airspeed, electric motor type, battery capacity, throttle input supply and electric motor controller. The efficiency of the propeller used is modeled based from UIUC [5]. The equation is given in Eq. (2).

$$P_a = \eta_{prop} P_0 \tag{2}$$

The power required is computed at the steady flight condition using Eq. (3).

$$P_R = \left(\frac{1}{2}\rho {V_\infty}^2 S_w C_D\right) V_\infty \tag{3}$$

The power available with 100% thrust setting and power required are shown in Figure 12.

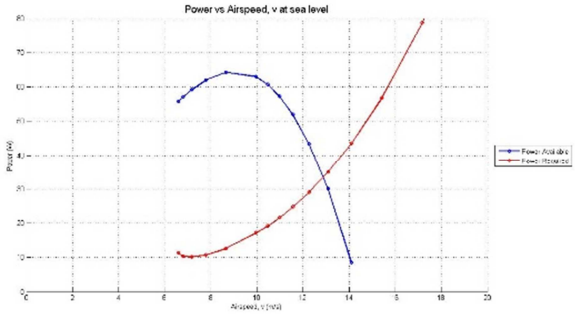

Figure 12: Power available (blue) and power required (red)

The results show that the limit of the electric motor that operates at 100% throttle is 33.5W at airspeed 12.87m/s. Several throttle inputs are also considered and the result shows that the minimum thrust is 60% throttle setting. The results are shown in Figure 13.

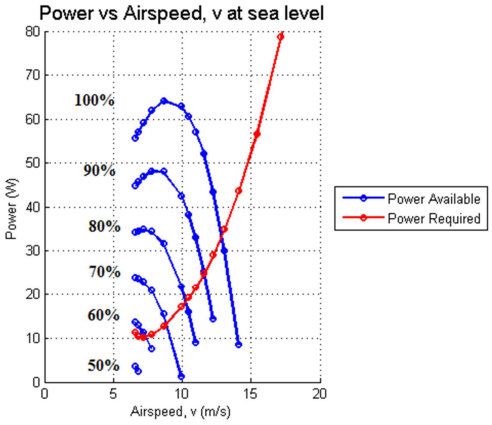

Figure 13: Various power available

6.0 STABILITY ANALYSIS

6.1 Static Stability

Static stability can be identified by observing the pitching, rolling and yawing moments as shown in Figure 9 and 10. The result shows that the aircraft is statically stable. This is proven according to Nelson (1998) reference book and the results is shown in equation (7), (8) and (9).

$$\frac{\partial C_{m_{cg}}}{\partial \alpha_e} < 0,\ C_{m,0_{cg}} > 0 \quad (7)$$

$$\frac{\partial C_{l_{cg}}}{\partial \beta} < 0,\ C_{l,0_{cg}} = 0 \quad (8)$$

$$\frac{\partial C_{n_{cg}}}{\partial \beta} > 0,\ C_{n,0_{cg}} = 0 \quad (9)$$

Besides, neutral point is calculated and it is located at 0.04 m behind center of gravity with static margin of 0.2271.

6.2 Dynamic Stability

The dynamic stability of the aircraft can be estimated using the analytical data obtained in the aerodynamic analysis. The linearized equations of motion approximate the longitudinal and lateral dynamic response [9]. The stability derivatives in the state space modeling and the sample equation are represented in Eq. (10). The state space modeling for longitudinal motion and lateral motion are as in Eq. (11), (12) and (13), respectively.

$$\dot{x} = Ax + B\eta_c \quad (10)$$

For longitudinal gliding flight,

$$\begin{bmatrix}\Delta\dot{u}\\ \Delta\dot{w}\\ \Delta\dot{q}\\ \Delta\dot{\theta}\end{bmatrix} = \begin{bmatrix}-0.3366 & 0.5583 & 0 & -9.810\\ -1.6011 & -11.4237 & 12.2537 & 0\\ 0.3261 & -2.5536 & -10.5841 & 0\\ 0 & 0 & 1 & 0\end{bmatrix}\begin{bmatrix}\Delta u\\ \Delta w\\ \Delta q\\ \Delta\theta\end{bmatrix} + \begin{bmatrix}0 & 0\\ -7.7199 & 0\\ -66.4509 & 0\\ 0 & 0\end{bmatrix}\begin{bmatrix}\Delta\delta_e\\ \Delta\delta_T\end{bmatrix} \quad (11)$$

For longitudinal powered flight,

$$\begin{bmatrix}\Delta\dot{u}\\ \Delta\dot{w}\\ \Delta\dot{q}\\ \Delta\dot{\theta}\end{bmatrix} = \begin{bmatrix}-0.5050 & 0.5583 & 0 & -9.810\\ -1.6011 & -11.4237 & 12.2537 & 0\\ 0.3261 & -4.3809 & -10.5841 & 0\\ 0 & 0 & 1 & 0\end{bmatrix}\begin{bmatrix}\Delta u\\ \Delta w\\ \Delta q\\ \Delta\theta\end{bmatrix} + \begin{bmatrix}0 & 0\\ -7.7199 & 0\\ -66.4509 & -0.0239\\ 0 & 0\end{bmatrix}\begin{bmatrix}\Delta\delta_e\\ \Delta\delta_T\end{bmatrix} \quad (12)$$

For lateral,

$$\begin{bmatrix}\Delta\dot{\beta}\\ \Delta\dot{p}\\ \Delta\dot{r}\\ \Delta\dot{\phi}\end{bmatrix} = \begin{bmatrix}-0.3426 & 0 & -0.9762 & 0.8006\\ -76.1768 & -43.3144 & 9.5746 & 0\\ 147.1112 & -1.2934 & -2.0016 & 0\\ 0 & 1 & 0 & 0\end{bmatrix}\begin{bmatrix}\Delta\beta\\ \Delta p\\ \Delta r\\ \Delta\phi\end{bmatrix} + \begin{bmatrix}0 & 0.2060\\ 3999.2809 & 22.8530\\ -44.7730 & -170.5637\\ 0 & 0\end{bmatrix}\begin{bmatrix}\Delta\delta_a\\ \Delta\delta_r\end{bmatrix} \quad (13)$$

MATLAB allows the transfer function and root locus plot for every single condition. The zero-pole plot is determined by obtaining the eigenvalues for matrix **A** in equation (11), (12) and (13). The results are shown in Table 3 and Figure 16 for longitudinal motion whereas Table 4 and Figure 17 for lateral motion.

Table 3: Eigenvalues for longitudinal motion

Eigenvalues for gliding flight	$\lambda_{phugoid} = -0.1591 \pm 0.6893i$ $\lambda_{short} = -9.7019 \pm 4.5943i$
Eigenvalues for powered flight	$\lambda_{phugoid} = -0.2364 \pm 0.7372i$ $\lambda_{short} = -9.7087 \pm 6.1624i$

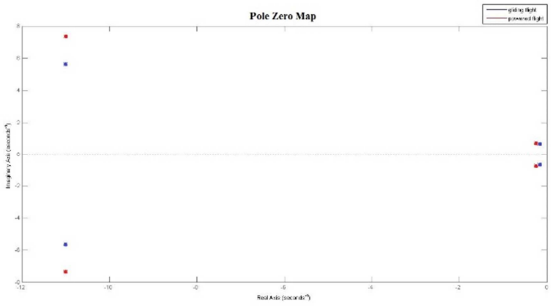

Figure 16: Pole zero plot for longitudinal motion

Table 4: Eigenvalues for lateral motion

Eigenvalues	$\lambda_{roll} = -43.1308$ $\lambda_{dutch\ roll} = -1.3418 \pm 12.1577i$ $\lambda_{spiral} = 0.1558$

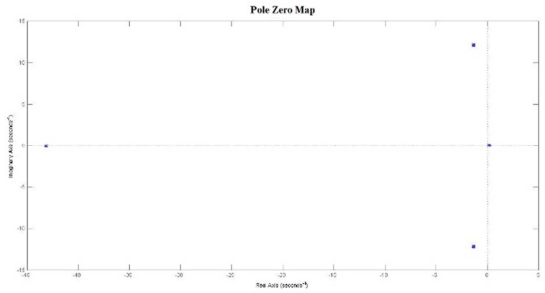

Figure 17: Pole zero plot for lateral motion

The results show that the longitudinal motion is dynamically stable. All poles are located at negative region. Whereas, the lateral motion is dynamically unstable due to the location of the spiral pole is located at positive region. This again can be proved by observing the initial condition applied to pitch, roll and yaw angles for 5°. The initial condition response is analyzed with MATLAB and results are shown in Figure 18.

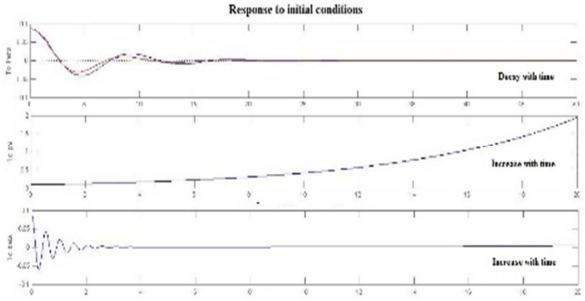

Figure 18: Response to initial conditions

7.0 PRELIMINARY DESIGN, DETAIL DESIGN AND FABRICATION

Figure 19 shows the three dimensional model of the aircraft. The fabrication is based from this design.

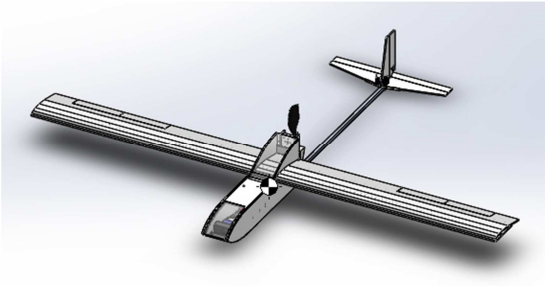

Figure 19: SolidWorks modeling of aircraft

The aircraft is fabricated by using simple fabrication method and low cost materials for example poly-foam, tape and wooden stick. Figure 20 shows the prototype.

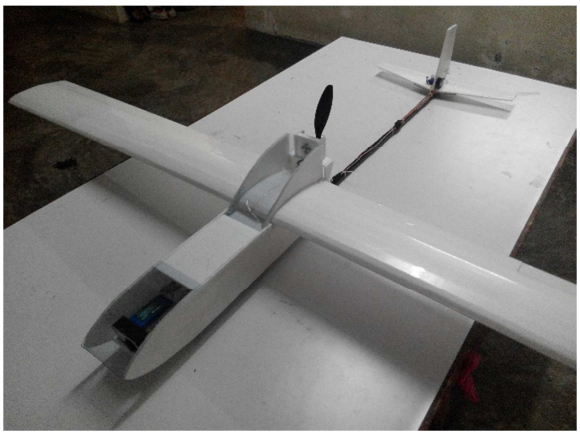

Figure 20: The prototype

8.0 FLIGHT TEST

Flight test is carried out and two main parameter pitch and roll angle are obtained using HK Mega Pilot 2.5 autopilot system. Besides, two autopilot modes are investigated, i.e. the manual mode and stabilizing mode where the augmented system is applied with the control setting listed in Table 5.

Table 5: PID setting in stabilizing mode

Servo Roll PID		Servo Pitch PID		Servo Yaw PID	
P	0.400	P	0.400	P	1.000
I	0.040	I	0.040	I	0.000
D	0.040	D	0.020	D	0.000

The results obtained for pitch angle is shown in Figure 21 (manual mode) and Figure 22 (stabilize mode).

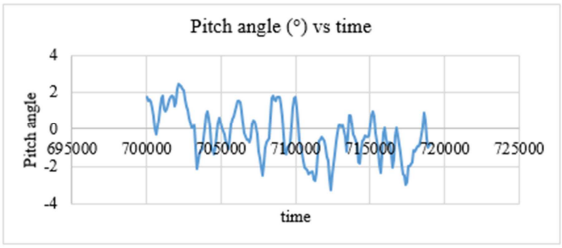

Figure 21: Pitch angle under manual mode

The results shows that the aircraft tend to stabilize itself at -1° pitch angle. The results show that the flight test correlates well with theoretical data.

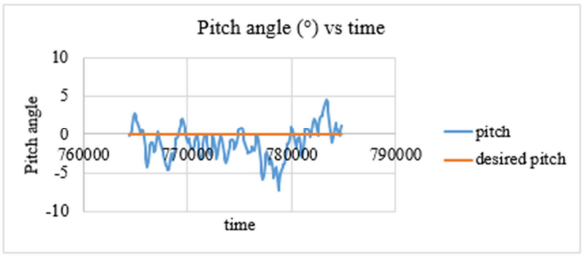

Figure 22: Pitch angle under stabilizing mode

With the stability augmentation, the results show that the reference PID setting does show improvement on the stabilizing response with moderate gust.

The roll motion is taken into consideration and Figure 23 shows roll motion with the manual mode and Figure 24 shows the roll motion with the stabilizing mode.

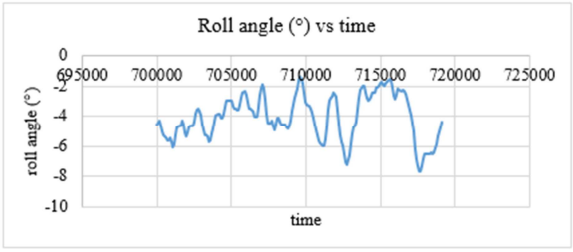

Figure 23: Roll motion under manual mode

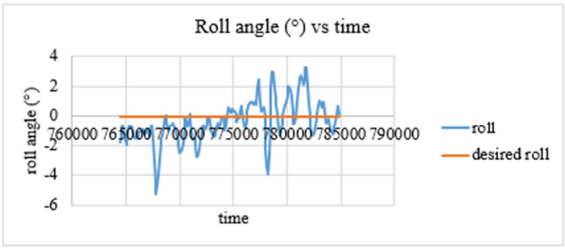

Figure 24: Roll motion under stabilizing mode

When comparing the responses, the stabilizing mode significantly improved the roll stability as compared to manual mode. Based on lateral dynamic stability, the unstable spiral eigenvalues would affect the lateral stability and this does correlate with roll motion under manual mode (Figure 23). However, as a augmented system is applied, the aircraft stabilize at zero roll angle in the present of moderate gust.

9.0 CONCLUSIONS

A proper design process is established by following the reference by Raymer (2006). Starting with the conceptual design of aircraft, the major sizing is simplified and determined accordingly. The design process follows the standard design process in which the analytical aerodynamic characteristics are determined, preliminary performance of the aircraft is identified and both static stability as well as dynamic stability are determined. The results are obtained and discussed. A flight test is conducted to understand the actual performance of the aircraft in manual and stabilize mode. It shows that the aircraft is able to achieve the required flying quality. The flying quality of the aircraft is further improved with the present of an auto-stabilization system. In general, the exercise of design and build of a small unmanned aircraft has achieved its objective. Further works are needed to study the performance and stability of the aircraft at various flying conditions.

REFERENCES

1. Parsch A., (2004). *AeroVironment FQM-151 Pointer*. Directory of U.S. Military Rockets and Missiles. Retrieved from: http://www.designation-systems.net/dusrm/m-151.html.
2. R/C Soaring Digest (2008): Olalla WA: B2Streamlines
3. Raymer D. P. (2006). *Aircraft Design: A Conceptual Approach*. American Institute of Aeronautics and Astronautics.
4. Capable Computing, (2015). *MotoCalc*. Retrieved from: www.motocalc.com
5. UIUC propeller database, (2015). In *UIUC Propeller Data Site*. Retrieved from: m-selig.ae.illinois.edu/props/propDB.html
6. Anderson J. D. (1999). *Aircraft Performance and Design*. The McGraw-Hill Companies Inc.
7. Anderson J. D. (1999). *Aircraft Performance and Design*. The McGraw-Hill Companies Inc.
8. Trips B., (2010). *Aerodynamic Design and Optimization of a Long Range Mini – UAV*. (Master of Science Thesis). Delft University of Technology.
9. Nelson R.C. (1998). *Flight Stability and Automatic Control*. The McGraw-Hill Companies. Inc.
10. Mark Drela, (1986), *XFOIL: An Analysis and Design System for Low Reynolds Number Airfoils*, Low-Reynolds Number Aerodynamics, Springer-Verlag Lec. Notes in Eng. 54.